# Consolidation-induced improvements in plate anchor capacity

Manuscript submitted to Canadian Geotechnical Journal

C. Wang; C. D. O'Loughlin; F. Bransby; P. Watson; Z. Zhou

**Ci WANG**
Centre for Offshore Foundation Systems, Oceans Graduate School
University of Western Australia
Perth, WA 6009, Australia
Email: ci.wang@research.uwa.edu.au

**Conleth D. O'LOUGHLIN**
Centre for Offshore Foundation Systems, Oceans Graduate School
University of Western Australia
Perth, WA 6009, Australia
Email: conleth.oloughlin@uwa.edu.au

**Fraser BRANSBY**
Centre for Offshore Foundation Systems, Oceans Graduate School
University of Western Australia
Perth, WA 6009, Australia
Email: fraser.bransby@uwa.edu.au

**Phil WATSON**
Centre for Offshore Foundation Systems, Oceans Graduate School
University of Western Australia
Perth, WA 6009, Australia
Email: phillip.watson@uwa.edu.au

**Zefeng ZHOU (corresponding author)**
Advanced modelling, Offshore energy
Norwegian Geotechnical Institute - NGI
Sandakerveien 140, Oslo Norway
Email: zefeng.zhou@ngi.no

Centre for Offshore Foundation Systems, Oceans Graduate School
University of Western Australia
Perth, WA 6009, Australia
Email: zefeng.zhou@uwa.edu.au

**Abstract**

Plate anchors are an attractive technology for mooring floating facilities as relative to piles, suction caissons and drag anchors they provide a much higher capacity relative to their mass. Plate anchors may experience an extreme loading event that will cause geotechnical failure, although they will still retain a residual capacity. The displacement associated with bringing the anchor to failure will induce excess pore pressures that initially reduce soil strength, but will dissipate over time, leading to regains in soil strength and hence anchor capacity. This paper considers the time scales and magnitude of this anchor capacity regain through a series of model scale experiments conducted in a geotechnical centrifuge. The experiments involved vertical loading of pre-embedded horizontally orientated circular anchors in normally consolidated kaolin clay. The results show that anchor capacity regain is a function of consolidation time and the level of resistance maintained on the anchor, with the longest consolidation time and highest maintained resistance leading to a capacity regain of approximately 60%. These capacity increases are described here using a simple hyperbolic function, which provides a basis for estimating the time needed for the residual anchor capacity to regain sufficient capacity following a movement event.

Keywords: Plate anchors, clay, centrifuge modelling, consolidation, offshore geotechnics, pore pressure, soil-structure interactions, softening.

## 1. INTRODUCTION

Floating energy production facilities experience environmental loading from the action of wind, waves and currents that is transmitted via the mooring lines to anchors in the seabed. As summarised in O'Loughlin et al. (2017), offshore anchors can be broadly categorised as either piles or plates, although gravity anchors (dead weights on the sea floor) are also considered for lower mooring line loads in shallow water. Pile anchors are slender steel tubes that are installed

by pile hammers (driven piles), pumping water from within the pile interior (suction caissons/piles), or by free-fall through the water column (dynamically installed piles). As shown in Figure 1, plate anchors are steel bearing plates that are installed either by dragging along the seabed (drag anchors), or by a retrievable follower, e.g. suction embedded plate anchors (SEPLAs, Wilde et al. 2001). SEPLAs (and other types of follower-embedded plate anchors) are installed at a controlled spatial location and to a known depth, which removes much of the uncertainty on soil strength – and hence anchor capacity – associated with drag-embedded plate anchors. As demonstrated in O'Loughlin et al. (2015), plate anchors are up to five times more efficient at resisting load than piles as they mobilise the soil in bearing rather than friction. These benefits present a compelling case for adopting plate anchors as an alternative to the more established pile anchor technology.

Plate anchors are typically designed to withstand a mooring line tension for a sea state with a return period of 100 years for offshore oil and gas facilities (DNV-OS-E301), and 50 years for offshore floating wind facilities (DNV-ST-0119), with different partial factors applied to the mooring line load depending on the loading conditions considered (DNV-RP-E302; Zhang et al. 2022). There is a growing body of work for various types of seabed infrastructure that shows geotechnical capacity increases over the design life, associated with consolidation-induced soil strength increases (Cocjin et al. 2014; White et al. 2017; Yuan et al. 2017; Zhou et al. 2020a), including work on plate anchors (e.g. Wong et al. 2012; Chen 2017; Zhou et al. 2020b). In some of these examples the foundation or infrastructure fails (from a geotechnical perspective; i.e. the maximum geotechnical capacity is exceeded), but retains a post-failure capacity that increases with time due to consolidation.

Should a plate anchor fail under an extreme loading condition, the anchor position and hence the local soil strength after the anchor has come to rest is of interest, as this controls the residual anchor capacity. The local strength will also be reduced initially due to the strain softening associated with the anchor movement during failure, but this will recover with time as the associated excess pore pressures dissipate. Hence, consideration of such events for an anchor requires an assessment of both the residual anchor capacity and its regain with time. This paper considers this problem through a series of experiments in which a plate anchor is moved through large displacements in a normally consolidated clay and the subsequent capacity measured after a period of time.

## 2. EXPERIMENTAL ARRANGEMENTS AND PROCEDURES

The experiments were performed in the 3.6 m diameter beam centrifuge at the National Geotechnical Centrifuge Facility, University of Western Australia, and involved vertical loading of horizontally orientated circular plate anchors that were pre-embedded in normally consolidated kaolin clay. The simplification of pre-embedding the anchor permits an assessment of anchor behaviour without consideration of installation effects. In addition, adopting a circular plate geometry allowed the results to be considered within the context of a broader database of experimental and numerical data for circular plates (e.g. Martin and Randolph, 2001; Zhou et al. 2020b). The tests involved an initial monotonic loading phase to establish the unconsolidated (large displacement) undrained anchor capacity, followed by a pause period that allowed for dissipation of excess pore pressures and a second monotonic loading phase to quantify the gain in anchor capacity due to consolidation in the pause period.

### 2.1 Model anchors and instrumentation

The experiments utilised circular model anchors with a diameter, $D$ = 40 mm and a thickness of 6 mm fabricated from either stainless steel or aluminium (see Figure 2). The anchor thickness was selected to accommodate a pore pressure transducer (with a measurement range of 400 kPa) in the centre of the top face of the anchor plate. The anchors were loaded by an actuator that was positioned such that the vertical axis of the actuator could reach a loading 'cap' that connected to the anchor via two 3 mm diameter stainless steel rods as shown in Figure 2. Anchor resistance was measured above the soil surface using a load cell (with a measurement range of 1 kN) located on the vertical axis of the actuator.

### 2.2 Sample preparation and characterization

The tests were conducted in a sample container (or 'strongbox') measuring 650 × 390 × 325 mm (length × width × depth) long using normally consolidated (Eckaolite) kaolin clay (with properties given in Table 1). Two-way drainage in the clay was facilitated by providing a hydraulic connection between a 10 mm base drainage layer of sand to the free water above the clay. The clay was mixed as a slurry in a vacuum mixer at a slurry with moisture content of 210% (equivalent to 2.85 times the liquid limit, $2.85w_{LL}$) for 24 hours before transferring to the strongbox. A 10 mm deep level clay layer was placed at the base of the strongbox before addition of the slurry or the anchors. This was designed to be of sufficient strength to support the anchors (see Figure 3a) and was prepared in a consolidometer under a final vertical stress

level of 30 kPa. The anchors were located as per the arrangement shown in Figure 3b and additional slurry added before transferring the sample to the centrifuge, where it was consolidated at the (anchor) testing acceleration level of 50*g* for 5 days, with additional slurry added after 18 hours to achieve a final sample height of ~ 210 mm (see Figure 3c).

During consolidation the anchor was free to move vertically with the settlement of the lower layer of preconsolidated clay, noting that this layer re-established a normally consolidated state in flight as the vertical effective stress due to the overlying clay was approximately 44 kPa (at 50*g*), i.e. greater than the 30 kPa preconsolidation stress. Lateral anchor movement was prevented by plastic ties that maintained the verticality of the anchor rods and their position within slots in the crossbeams that spanned the width of the strongbox (see Figure 3b).

After consolidation was considered essentially complete (as assessed from free-field pore pressure measurements within the sample) T-bar penetrometer tests (Stewart & Randolph, 1991) were undertaken to quantify the intact and remoulded undrained shear strength, $s_{ui}$ and $s_{ur}$, using a model scale T-bar penetrometer with a diameter of 5 mm and a length of 20 mm. The T-bar was advanced at a velocity, $v$ = 2 mm/s, such that the dimensionless velocity, $V = vd/c_v = 52$ (where $d$ = 5 mm and the coefficient of vertical consolidation, $c_v$ = 6.1 m$^2$/year, taken at a stress level equivalent to that at the mid-depth of the sample), such that the response can be considered undrained (House et al. 2001). Depth profiles of $s_u$ are provided in Figure 4a, where $s_u$ was determined from the measured penetration resistance using a T-bar factor, $N_{T\text{-bar}}$ = 10.5 (Martin and Randolph, 2006).

T-bar tests were conducted over the 15-day duration of the anchor tests, and indicate that the sample strengthened slightly from an undrained shear strength ratio, $s_u/\sigma'_{v0}$ = 0.22 to 0.25 over the course of the testing. Cyclic remoulding stages were included in each T-bar test, where the T-bar was displaced vertically by ±30 mm (i.e. 6 T-bar diameters, 6*d*) for 20 cycles. The degradation in soil strength with cycle number is shown in Figure 4b and indicates a soil sensitivity (based on penetration resistance) in the range $S_t$ = 2.5 to 2.7. Also shown in Figure 4b is the strength degradation exponential decay model of Einav and Randolph (2005), but where the initial cycle number is defined as $N$ = 0.25 (Randolph et al. 2007), for deducting degradation parameters from cyclic penetration tests:

$$\frac{s_{u,N}}{s_{u,i}} = \delta_{rem} + (1 - \delta_{rem}) e^{\left(-3\left(N - \frac{0.25}{N_{95}}\right)\right)} \quad (1)$$

where $s_{u,N}$ is the undrained shear strength at cycle number, $N$; $s_{u,i}$ in the intact undrained shear strength measured during the initial pass of the T-bar (at $N$ = 0.25, $\delta_{rem}$ is the ratio of the fully

remoulded undrained strength to the initial undrained shear strength (i.e. $\delta_{rem} = 1/S_t$) and $N_{95}$ is the number of cycles required for 95% reduction in su from the intact to the remoulded condition. The best agreement with the measured T-bar response is obtained using $\delta_{rem} = 0.37$ and $N_{95} = 5.5$.

In addition to these standard T-bar tests, a series of T-bar tests involving fixed position pauses during penetration were undertaken to provide a basis for understanding soil strength changes due to consolidation. Figure 4a also includes selected results from these T-bar tests, with the localised soil strengths indicated by the post-pause (20 to 60%) increases in penetration resistance. These results are discussed later in the paper given the relevance of this data to the anchor response.

### 2.3 Experimental arrangement and procedures

Figure 5 shows the experimental arrangement. The anchors were located at an embedment depth of approximately 190 mm (4.75$D$) with a minimum clear distance between anchors of 97 mm (2.4$D$) and to strongbox walls of 90 mm (2.25$D$). This lateral spacing exceeds the lateral extent for a localised failure mechanism (a maximum of 0.37$D$ beyond the edge of the plate, Martin and Randolph, 2001), such that interaction and boundary effects may be considered negligible. The rigid base was initially 20 mm (0.5$D$) from the underside of the anchor, although this reduced to between 4 and 11 mm due to the additional settlement caused by consolidation in the centrifuge. The close proximity of the rigid base is likely to introduce a mechanism constraint during the initial capacity mobilisation stage, but is not considered to affect the steady state anchor resistance or the capacity response after consolidation, as the anchor was displaced vertically by one anchor diameter before pausing for consolidation.

As noted earlier, each anchor test involved an initial phase of monotonic loading followed by a consolidation stage and a final monotonic loading phase. Both monotonic phases involved operating the actuator in displacement control at a penetration velocity, $v$ = 0.75 mm/s, such that $V = vD/c_v = 139$ (adopting $c_v = 6.8$ m$^2$/year taken at the initial vertical effective stress level at the anchor test depth). This dimensionless velocity exceeds the threshold $V = 30$ for undrained behaviour suggested by numerous experimental studies on different penetrometer and foundation geometries (e.g. House et al. 2001; Erbrich, 2005; Lee and Randolph, 2011; Chow et al., 2020a; Chow et al., 2020b; Wroth et al., 2022; Roy et al., 2022). The initial monotonic loading involved a vertical movement of 40 mm (i.e. one anchor diameter), such that the anchor embedment depth after this movement was 3.75$D$, sufficient for the plate to be considered deep

(from a capacity mobilisation perspective) (e.g. Wang et al., 2010; Yu et al., 2011; Wang and O'Loughlin, 2014 and O'Loughlin et al., 2017). In the second monotonic loading stage, the anchor was moved through a distance that was sufficient to observe the post-consolidated peak anchor resistance (typically 20 mm, 0.5$D$). The consolidation stage involved either maintaining the anchor embedment depth (achieved by locking the actuator in position) or by applying an upward anchor loading equal to approximately 20% of that measured at the end of the initial monotonic loading (which required that the actuator was operated in load control). The anchor test programme is summarised in Table 2.

## 3. RESULTS AND DISCUSSION

### 3.1 Undrained-unconsolidated capacity

The responses measured during the initial monotonic loading stage are provided in **Figure 6.** The data are presented as $q_{u,u}/s_u^*$, where $q_{\mathrm{u,u}}$ is the net undrained unconsolidated anchor resistance, calculated as the net anchor load (i.e. the measured load minus the estimated friction from the rods and the submerged weight of the anchor/rod system) divided by the projected anchor area ($A = \pi D^2/4$), and $s_u^*$ is the initial undrained shear strength at the depth of the instantaneous centre of the anchor adjusted to account for the different strain rates associated with the anchor movement and the T-bar penetration. This strain rate adjustment was undertaken using a strain-rate power law (Biscontin and Pestana, 2001):

$$s_u^* = s_{u,ref}\left(\frac{v/D}{(v/D)_{ref}}\right)^{\beta} \quad (2)$$

where $s_{\mathrm{u,ref}}$ is the reference T-bar strength taken as $s_{\mathrm{u,i}}$, β is a strain rate parameter and $v/D$ and $(v/D)_{\mathrm{ref}}$ are assumed to be proportional to the strain rates associated with the anchor and T-bar movements. As noted earlier, the T-bar and anchor velocities were selected such that the dimensionless velocity for drainage, $V$ was approximately the same in each case. This achieves the same drainage response but results in differing strain rates; $v/D$ = 0.019 s$^{-1}$ for the anchor, approximately 20 times lower than $(v/D)_{\mathrm{ref}}$ = 0.4 s$^{-1}$ for the T-bar. Adopting β = 0.05 (Wang et al. 2023) in Eq. 2 results in a 14% reduction in the T-bar measured soil strength, which is used in the normalisation of the anchor penetration resistance in Figure 6.

Figure 6 shows that anchor resistance rises to a peak value in the range $q_{u,u}/s_u^*$ = 14.6 to 18.5 after approximately 2 mm (0.05$D$) and 3.2 mm (0.08$D$) of anchor movement. After an anchor movement of 0.5$D$ to 0.8$D$, anchor resistance reduces to an average $q_{u,u}/s_u^*$ = 10.5, identical

to the $N_{\text{T-bar}}$ = 10.5 used to calculate the initial undrained shear strength from the T-bar penetrometer resistance, inferring a similar amount of strain softening for the T-bar and the plate. The reduction to a stabilised $q_{u,u}/s_u^*$ = 10.5 in each test is due to the strain softening associated with the vertical anchor movement, and implies that the specific modelling conditions associated with model construction, spin-up and initial consolidation were erased by the 1D of vertical movement.

### 3.2 Consolidated capacity

The response during maintained loading and the subsequent monotonic response are shown in Figure 7. Anchor resistance, $q$, is normalised by both the initial undrained shear strength at the current anchor depth (adjusted for strain rate), $s_u^*$, (Figure 7a) and by the anchor resistance at the end of the initial monotonic loading stage, $q_{\text{u,u}}$ (Figure 7b). Normalised anchor displacements, $\Delta z/D$, are relative to the anchor depth at the beginning of the final monotonic loading stage. Figures 7a and 7b show results from tests where the anchor load was maintained for consolidation periods of either 0.15 or 48 hours. The maintained load was either approximately 25% of that measured at the end of the unconsolidated, undrained event (for Test 1 and 2) or 0 kPa (in Test 3). In each test the anchor moved vertically downwards during the maintained load phase. As explained in Wang et al. (2023), anchor movement in the initial monotonic loading causes excess pore pressure development in the soil beneath the anchor. Over time this soil consolidates, leading to a volume reduction that causes the anchor to move vertically downwards.. The smaller vertical movement in Test 2 relative to Test 3 (both maintained for 48 hours) is due to the difference in the magnitude of the maintained anchor load, with the higher load in Test 2 tending to offset the consolidation-induced settlement. The lower vertical movement in Test 1 than in Test 2 is consistent with the significantly different consolidation times in the two tests. The post-consolidation monotonic response indicates anchor capacity increases (defined as the ratio of the consolidated anchor capacity, $q_{\text{c,u}}$, to the initial residual anchor capacity, $q_{\text{u,u}}$) in the range, $q_{\text{c,u}}/q_{\text{u,u}}$ = 16% to 61%.

Figure 7c and 7d shows equivalent data from tests where the anchor position was fixed for consolidation periods in the range 0.375 to 48 hours (during which the mobilised soil resistance reduced). Consistent with the load-controlled consolidation results on Figure 7a and 7b, the increase in anchor capacity is higher for longer consolidation periods, with increases in the range $q_{\text{c,u}}/q_{\text{u,u}}$ = 30% to 63%. In all tests (fixed position and maintained load) anchor capacity

reduces with additional displacement, but remains at $q/q_{u,u} > 1$ even after an additional $0.5D$ of anchor displacement.

### 3.3 Anchor capacity and soil strength gains with time

The complete data set of peak soil resistance versus pause duration is shown in Figure 8 and includes tests where the anchor resistance was maintained at $q = 0.25q_{u,u}$ and at $q = 0$ kPa, and also tests where the anchor position rather than the load was maintained. Figure 8 indicates that anchor capacity increases with consolidation time, with a maximum increase of approximately 60% relative to the softened unconsolidated anchor capacity. Assuming a typical anchor capacity factor of $N_c = 14$ is adopted in design (for a circular plate, e.g. see Wang and O'Loughlin, 2014), the dimensionless time required for anchor capacity factor to return to the design value (i.e. to mobilise a consolidation-induced capacity increase of 14/10.5 = 1.33) is around $T = 0.3$. This corresponds to a time of approximately 0.1 to 1 years for an anchor with a diameter of about 4.4 m in clay with a range of $c_v$ values from 1 to 10 m$^2$/yr. However, consideration also needs to be given to the initial undrained shear strength profile, as vertical components of anchor displacement is likely to move the anchor into soil with a lower strength.

Also shown on Figure 8 are data from the T-bar tests with consolidation ('pause') periods (see Figure 2a), where the change in T-bar resistance is also expressed as $q_{c,u}/q_{u,u}$, with $q_{c,u}$ quantifying the consolidated T-bar resistance and $q_{u,u}$ the initial T-bar resistance. The capacity increases inferred from the T-bar tests are consistent with those from the anchor tests, with a maximum increase of approximately 60% in either case, indicating an equivalent amount of excess pore pressure induced by steady state movement of the anchor and the T-bar. This suggests that T-bar tests – conducted offline in samples retrieved in the geotechnical investigation to avoid extending investigation durations and costs – with such pause periods might offer a site-specific approach to measuring this capacity increase.

The three anchor tests at $T = 21.5$ ($t = 48$ hrs) in which either the position was fixed or anchor resistance was controlled ($q = 0.25q_{u,u}$ and $q = 0$ kPa) all show different post consolidated capacities. In the fixed position test the mobilised soil resistance varied with time (as explained further in Wang et al. 2023), but was on average equal to approximately $0.75q_{u,u}$. The post-consolidated anchor capacity increases (relative to the unconsolidated anchor capacity, $q_{u,u}$) by approximately 30% in the test where $q = 0$ kPa was maintained, but by approximately 61% in the test where $q = 0.25q_{u,u}$ was maintained, and by approximately 63% in the fixed displacement test. Hence, the post consolidated anchor capacity is controlled not only by the excess pore

pressure generated during undrained shearing, but also by the total stress applied during the maintained loading phase.

The degree of consolidation can be approximated from both the anchor and T-bar data by expressing the increase in anchor capacity or T-bar resistance as a ratio of the maximum change:

$$\boldsymbol{U = \frac{q_{c,u} - q_{u,u}}{q_{c,u,max} - q_{u,u}}} \quad (5)$$

where $q_{c,u,max}$ is the maximum consolidated anchor capacity and the maximum consolidated undrained T-bar resistance. As noted by Randolph (2003), the assumption that capacity and strength changes are proportional to the degree of consolidation (i.e. Equation 5) ignores other effects that take place as the soil strength or anchor capacity is mobilised. However, as this approach has been used successfully for dynamically installed anchors (Richardson et al. 2009) and suction caissons (Jeanjean 2006), its use here is considered reasonable. The degree of consolidation for the anchor and T-bar data are shown on Figure 9 together with the Osman & Randolph (2012) analytical solution for a deeply buried cylinder, which is approximated here by the following hyperbolic function, often used to describe consolidation responses (e.g. Gourvenec et al. 2014; Feng & Gourvenec 2015):

$$\boldsymbol{U = 1 - \frac{1}{1 + \left(T/T_{50}\right)^{m}}} \quad (6)$$

where $T_{50}$ is the dimensionless time associated with 50% consolidation (i.e. $U$ = 0.5) and the exponent, m, controls the steepness of the 'backbone' consolidation curve. Equation 6 provides best agreement with the Osman and Randolph (2012) solution using $T_{50}$ = 1.4 and $m$ = 0.68. The T-bar data are seen to agree well with the Osman and Randolph (2012) solution, although a slightly improved match is obtained using $T_{50}$ = 1.0 and $m$ = 0.9. The T-bar data are evidently offset from the anchor data, with Equation 6 providing a good match using $T_{50}$ = 0.3 and (the same) $m$ = 0.9. The lower $T_{50}$ for the anchor data is consistent with the faster consolidation expected for the three-dimensional consolidation around a circular plate. The reduction in $T_{50}$ (between the T-bar and anchor data) is by a factor of 3.3, broadly consistent (albeit slightly lower) than the ~5 fold reduction between circular and strip shallow foundations deduced from numerical analyses (Gourvenec et al. 2014), which may be due to the different geometry of the T-bar compared to the strip foundation (in elevation view). The different $T_{50}$ and $m$ values for the T-bar and plate data indicate that adjustments to $T_{50}$ = 1.4 and $m$ = 0.68 may be required for other anchor geometries. Additional data for other plate anchor geometries in different soils would provide further certainty in this regard.

Figure 9 suggests $T_{50} \sim 0.3$ based on anchor capacity changes, whereas anchor pore pressure dissipation data measured at the anchor face shown on Figure 10 (for two 48 hour tests) indicates $T_{50} \sim 0.05$, i.e. approximately six times faster. However, as shown experimentally in Wang et al. (2023) and numerically by Gourvenec and Randolph (2009) the far-field consolidation, which governs anchor capacity changes, progresses slower.

## 4. CONCLUDING REMARKS

This paper describes a set of centrifuge model-scale experiments on pre-embedded circular plate anchors in normally consolidated clay that quantify anchor capacity recovery due to consolidation after a large anchor movement. These tests consider the scenario in which anchor failure has occurred, for which it is important to understand how the magnitude of the residual anchor capacity changes over time.

The data show anchor capacity increases of up to about 60%, which for the kaolin clay investigated here, are sufficient to more than compensate for the capacity reduction associated with strain-softening. Capacity regains are shown to be controlled not only by the duration of consolidation, but also by the level of soil resistance maintained on the anchor during consolidation. This is because the maintained anchor loads add a total-stress induced pore pressure component (to the shear-induced pore pressures developed during the initial anchor movement), which results in a higher effective stress and hence increased soil strength after consolidation.

The time dependence of the anchor (and T-bar) strength gains observed in the experiments was shown to be described well by a simple hyperbolic consolidation equation. Furthermore, the amount of soil strength increase after full reconsolidation generated in the anchor tests was almost identical to the increase obtained during T-bar tests in which the T-bar was held in a fixed position to allow consolidation and then moved downwards. This suggests that such tests could potentially provide a means for making site-specific measurement of such capacity increases, thereby allowing both the magnitude and duration of anchor strength changes to be quantified.

## 5. ACKNOWLEDGEMENTS

The first author acknowledges her research studentship support from the ARC Industrial Transformation Research Hub for Offshore Floating Facilities and the University of Western Australia. This work was supported by the ARC Industrial Transformation Research Hub for

Offshore Floating Facilities which is funded by the Australia Research Council, Woodside Energy, Shell, Bureau Veritas and Lloyds Register (Grant No. IH140100012). The third author acknowledges the support of Fugro, provided via the Fugro Chair in Geotechnics at UWA. The fourth author leads the Shell Chair in Offshore Engineering research team at The University of Western Australia, which is sponsored by Shell Australia. The corresponding author acknowledges his research support from Norwegian geotechnical Institute – NGI.

## 6. NOTATION

$c_v$ coefficient of vertical consolidation

$d$ T-bar diameter

$D$ plate diameter

$G_s$ specific gravity

$w_{LL}$ liquid limit

$m$ parameter for dissipation rate

$N$ cycle number

$N_c$ anchor capacity factor

$N_{T\text{-}bar}$ T-bar factor

$N_{95}$ 95% reduction in operative strength from the intact to remoulded condition

$w_{PL}$ plastic limit

$q$ anchor resistance

$q_{u,u}$ undrained unconsolidated anchor resistance

$q_{c,u}$ consolidated undrained anchor resistance

$q_{c,u,max}$ maximum consolidated anchor capacity

$s_u$ undrained shear strength

$s_u^*$ strain rate adjusted initial undrained strength

$s_{u,c}$ consolidated undrained soil strength

$s_{u,i}$ initial undrained shear strength measured during the initial pass of the T-bar (at $N = 0.25$)

| | |
|---|---|
| $s_{u,c,max}$ | maximum consolidated undrained shear strength |
| $s_{u,N}$ | undrained shear strength at cycle number, N |
| $s_{u,ref}$ | reference T-bar strength (taken as $s_{u,i}$) |
| $S_t$ | soil sensitivity |
| $t$ | time |
| $T$ | dimensionless time |
| $T_{50}$ | dimensionless time associated with 50% consolidation |
| $u_e$ | excess pore pressure |
| $u_{e,i}$ | initial excess pore pressure |
| $U$ | degree of consolidation |
| $v$ | penetration velocity |
| $V$ | dimensionless velocity |
| $\triangle z$ | anchor displacement |
| $z$ | depth |
| $\beta$ | strain rate parameter |
| $\gamma'$ | effective unit weight of soil |
| $\delta_{rem}$ | fully remoulded strength ratio |
| $\kappa$ | gradient of unload-reload line (URL) |
| $\lambda$ | gradient of normal compression line (NCL) |
| $\sigma'_{v0}$ | initial vertical effective stress |
| $\sigma'_{veqm}$ | equilibrium vertical effective stress |
| $c_v$ | coefficient of vertical consolidation |
| $d$ | T-bar diameter |
| $d_e$ | equivalent diameter (T-bar) |
| $D$ | plate diameter |

| | |
|---|---|
| $G_s$ | specific gravity |
| $w_{LL}$ | liquid limit |
| $m$ | parameter for dissipation rate |
| $N$ | cycle number |
| $N_c$ | anchor capacity factor |
| $N_{T\text{-}bar}$ | T-bar factor |
| $N_{95}$ | 95% reduction in operative strength from the intact to remoulded condition |
| $w_{PL}$ | plastic limit |
| $q$ | anchor resistance |
| $q_{u,u}$ | undrained unconsolidated anchor resistance |
| $q_{c,u}$ | consolidated undrained anchor resistance |
| $q_{c,u,max}$ | maximum consolidated anchor capacity |
| $s_u$ | undrained shear strength |
| $s_u^*$ | strain rate adjusted initial undrained strength |
| $s_{u,c}$ | consolidated undrained soil strength |
| $s_{u,i}$ | initial undrained shear strength measured during the initial pass of the T-bar (at $N = 0.25$) |
| $s_{u,c,max}$ | maximum consolidated undrained shear strength |
| $s_{u,N}$ | undrained shear strength at cycle number, N |
| $s_{u,ref}$ | reference T-bar strength (taken as $s_{u,i}$) |
| $s_{ur}$ | remoulded undrained shear strength |
| $S_t$ | soil sensitivity |
| $t$ | time |
| $T$ | dimensionless time |
| $T_{50}$ | dimensionless time associated with 50% consolidation |
| $u_e$ | excess pore pressure |

$u_{e,i}$ initial excess pore pressure

$U$ degree of consolidation

$v$ penetration velocity

$V$ dimensionless velocity

## 7. DATA AVAILABILITY STATEMENT

Data generated or analyzed during this study are available from the corresponding author upon reasonable request.

## 8. COMPETING INTERESTS STATEMENT

The authors declare there are no competing interests.

## 9. REFERENCES

Biscontin, G., and Pestana, J. M. (2001). Influence of peripheral velocity on vane shear strength of an artificial clay. *ASTM Geotechnical Testing Journal*, 24(4), 423-429.

Cocjin, M. L., Gourvenec, S. M., White, D. J. and Randolph, M. F. (2014). Tolerably mobile subsea foundations-observations of performance. *Géotechnique*, 64(11), 895-909. https://doi.org/10.1680/geot.14.P.098

Chow, S. H., Bienen, B., and Randolph, M.F. (2020a). Rapid penetration of spudcans in sand. In Proceedings of the 4th International Symposium on Frontiers in Offshore Geotechnics, Austin, Nov., pp. 49–74

Chow, S. H., Diambra, A., O'Loughlin, C. D., Gaudin, C., and Randolph, M. F. (2020b). Consolidation effects on monotonic and cyclic capacity of plate anchors in sand. *Géotechnique*, 70(8), 720-731.

Chen, J. (2017). *Centrifuge model study on pull-out behaviour of suction embedded plate anchor*. PhD thesis, the National University of Singapore.

Chung, S. F., Randolph, M. F. and Schneider, J. A. (2006). "Effects of penetration rate on penetrometer resistance in clay." Journal of Geotechnical and Geoenvironmental Engineering, 132(9), pp. 1188–1196.

DNV (Det Norske Veritas) (2021). DNV-OS-E301: Recommended practices: position

mooring. DNV

DNV (Det Norske Veritas) (2021). DNV-ST-0119: Floating wind turbine structures. DNV

DNV (Det Norske Veritas) (2021). DNV-RP-E302: Recommended practices: design and installation of plate anchors in clay. DNV

Erbrich, C.T. (2005). Australian frontiers – Spudcans on the edge. In Proceedings of the 1st International Symposium on Frontiers in Offshore Geotechnics, Perth, Aust., pp. 49–74

Einav, I. and Randolph, M. F. (2005). Combining upper bound and strain path methods for evaluating penetration resistance. *International Journal for Numerical Methods in Engineering*, No. 14, 1991-2016. https://doi.org/10.1002/nme.1350

Feng, X. & Gourvenec, S. (2015). Consolidated undrained load carrying capacities of mudmats under combined loading in six degrees-of-freedom. *Géotechnique*, 65(7), 563–575. https://doi.org/10.1680/geot.14.P.090

Lee, J., and Randolph, M. (2010). Penetrometer-based assessment of spudcan penetration resistance. Journal of Geotechnical and Geoenvironmental Engineering 137(6): 587- 596

Gourvenec, S., Vulpe, C., and Murphy, T. G. (2014). A method for predicting the consolidated undrained bearing capacity of shallow foundations. *Géotechnique* 64, No. 3, 215–225. https://doi.org/10.1680/geot.13.P.101

Gourvenec, S. and Randolph, M. F. (2009). Effect of foundation embedment and soil properties on consolidation response. *Proceedings of the International Conference on Soil Mechanics and Geotechnical Engineering* (ICSMGE), Alexandria, Egypt, pp. 638–64.

House, A., Olivera, J. R. M. S., and Randolph, M. F. (2001). Evaluating the coefficient of consolidation using penetration tests. *International Journal of Physical Modelling in Geotechnics*, 3, 17–25. https://doi.org/10.1680/ijpmg.2001.010302

Jeanjean, P. (2006). Setup characteristics of suction anchors for soft Gulf of Mexico clays: Experience from field installation and retrieval. *Proc.,Offshore Technology Conf., Offshore Technology Conference*, Houston. https://doi.org/10.4043/18005-MS

Lehane, B. M., O'Loughlin, C. D., Gaudin, C. & Randolph, M. F. (2009). Rate effects on penetrometer resistance in kaolin. *Géotechnique*，59 (1), 41–52.

Martin, C. M. & Randolph, M. F. (2001). Application of the lower bound and upper bound theorems of plasticity to collapse of circular foundation. *Computer methods and advances in geomechanics* (eds C. Desai, T. Kundu, S. Harpalani, D. Contractor and J. Kemeny), vol. 2, pp. 1417–1428. Boca Raton, FL, USA: CRC Press/Balkema.

Martin, C. M. & Randolph, M. (2006). Upper-bound analysis of lateral pile capacity in cohesive soil. *Géotechnique* 56 (2), 141–145. https://doi.org/10.1680/geot.2006.56.2.141.

O'Loughlin, C.D., White. D.J. and Stanier, S. (2015). Novel Anchoring Solutions for FLNG - Opportunities Driven by Scale. *Proceedings of the 2015 Offshore Technology Conference*. Paper number OTC-26032.

O'Loughlin, C. D., White, D. J. and Stanier, S. A. (2017). Plate anchors for mooring floating facilities - a view towards unlocking cost and risk benefits. *Offshore Site Investigation and Geotechnics 2017 Conference Proceedings*. United Kingdom, Vol. 2. 978-986. https://doi.org/10.3723/OSIG17.978

Osman, A.S. & Randolph (2012). Analytical solution for the consolidation around a laterally loaded pile. *International Journal of Geomechanics*, 12(3):199-208. http://dx.doi.org/10.1061/(ASCE)GM.1943-5622.0000123

Randolph, M. F., Low, H. E. and Zhou, H. (2007). In situ testing for design of pipeline and anchoring systems. *Proceedings of the 6th International Conference on Offshore Site Investigation and Geotechnics: Confronting New Challenges and Sharing Knowledge* London, UK., 251–262.

Richardson, M. D., O'Loughlin, C. D., Randolph, M. F. and Gaudin C. (2009). Setup Following Installation of Dynamic Anchors in Normally Consolidated Clay. *Journal of Geotechnical and Geoenvironmental Engineering*, 135(4), 487–496.

Roy, A., Chow, S. H., Randolph, M. F. and O'Loughlin, C. D. (2022). Consolidation effects on uplift capacity of shallow horizontal plate anchors in dilating sand. *Géotechnique*, 72(11), 957-973

Stewart, D. P. and Randolph, M. F. (1991). A new site investigation tool for the centrifuge. *Proceedings of the International Conference on Centrifuge Modelling*, Centrifuge '91, Boulder, Colorado, USA, 531–538.

Wang, D., Hu, Y., and Randolph, M.F. (2010). Three-dimensional large deformation finite-

element analysis of plate anchors in uniform clay. Journal of Geotechnical and Geoenvironmental Engineering, 136(2): 355–365. doi:10.1061/(ASCE) GT.1943-5606.0000210.

Wang, D. and O'Loughlin, C. D. (2014). Numerical study of pull-out capacities of dynamically embedded plate anchors. *Canadian Geotechnical Journal*, 51(11), 1263-1272. https://doi.org/10.1139/cgj-2013-0485

Wang, C., O'Loughlin, C. D., Bransby, M. F., Watson, P. and Zhou, Z. (2023). Complex time-dependent processes influencing offshore foundations in clay: an experimental study on plate anchors. Géotechnique, under review.

Wong, P., Gaudin, C., Randolph, M., Cassidy, M. and Tian, Y. (2012). Performance of suction embedded plate anchors in permanent mooring applications. *Proceedings of The Twenty-second International Offshore and Polar Engineering Conference 2012*. USA. 640-645.

Wroth, H.M., Bransby, M.F., and O'Loughlin, C. D., (2022). Using near-surface CPT data to predict foundation skirt embedment in partially drained carbonate sands. In Proceedings of the 5th International Symposium on Cone Penetration Testing (CPT'22), Italy, June., pp. 1149–1155

White, DJ, Clukey EC, Randolph MF, Boylan NP, Bransby MF, Zakeri A, Hill AJ, Jaeck C. (2017). The state of knowledge of pipe-soil interaction for on-bottom pipeline design. OTC 27623, *Proc. Offshore Technology Conference*, Houston. https://doi.org/10.4043/27623-MS

Wilde, B., True, H and Fultonb, T. (2001). Field testing of suction embedded plate anchors. *Proceedings of the 11th International Offshore and Polar Engineering Conference*. Paper Number: ISOPE-I-01-208.

Yu, L., Liu, J., Kong, X.-J. and Hu, Y. (2011). Numerical study on plate anchor stability in clay. Géotechnique, 61(3), 235-246.

Yuan, F., White, D. J., and O'Loughlin, C. D. (2017). The evolution of seabed stiffness during cyclic movement in a riser touchdown zone on soft clay. *Géotechnique*, 67(2), 127-137. https://doi.org/10.1680/jgeot.15.P.161

Zhang, W., Zhou, Z., Pardhan, D. L., Wang, P., Jin, H. (2022). Design considerations of drag anchors in cohesive soil for floating facilities in the South China sea. *Marine Structures*,

81-103101. https://doi.org/10.1016/j.marstruc.2021.103101

Zhou, Z., White, D. J. and O'Loughlin, C.D. (2020a). The changing strength of carbonate silt: parallel penetrometer and foundation tests with cyclic loading and reconsolidation periods. *Canadian Geotechnical Journal*, 57 (11),1664-1683. https://doi.org/10.1139/cgj-2019-0066

Zhou, Z., O'Loughlin, C. D., White, D. J., Stanier, S. A. (2020b). Improvements in plate anchor capacity due to cyclic and maintained loads combined with consolidation. *Géotechnique*, 70(8), 732-749. https://doi.org/10.1680/jgeot.19.TI.028

## 10. FIGURE CAPTIONS

Figure 1 Offshore anchors and mooring systems

Figure 2 Model anchor and instrumentation

Figure 3 Sample preparation and anchor installation: (a) consolidation of lower clay layer; (b) anchor installation; (c) sample consolidation

Figure 4 T-bar test data: (a) undrained shear strength profiles; (b) degradation in undrained shear strength during cyclic remoulding ($z$ = 105 mm)

Figure 5 Experimental arrangement

Figure 6 Anchor response during initial undrained monotonic loading

Figure 7 Anchor capacity increases after consolidation: (a) and (b) tests where the anchor resistance was fixed during consolidation; (c) and (d) tests where the anchor displacement was fixed during consolidation ((a) and (c) show anchor resistance normalised by undrained shear strength, whereas (b) and (d) show anchor resistance normalised by that at the end of the initial monotonic loading)

Figure 8 Changes in anchor capacity and soil strength after various consolidation periods

Figure 9 Degree of consolidation for anchor and T-bar tests

Figure 10 Consolidation progression as estimated from anchor capacity data and measured pore pressure response

## 11. TABLE CAPTIONS

Table 1 Geotechnical properties of Eckaolite kaolin clay

Table 2 Test programme

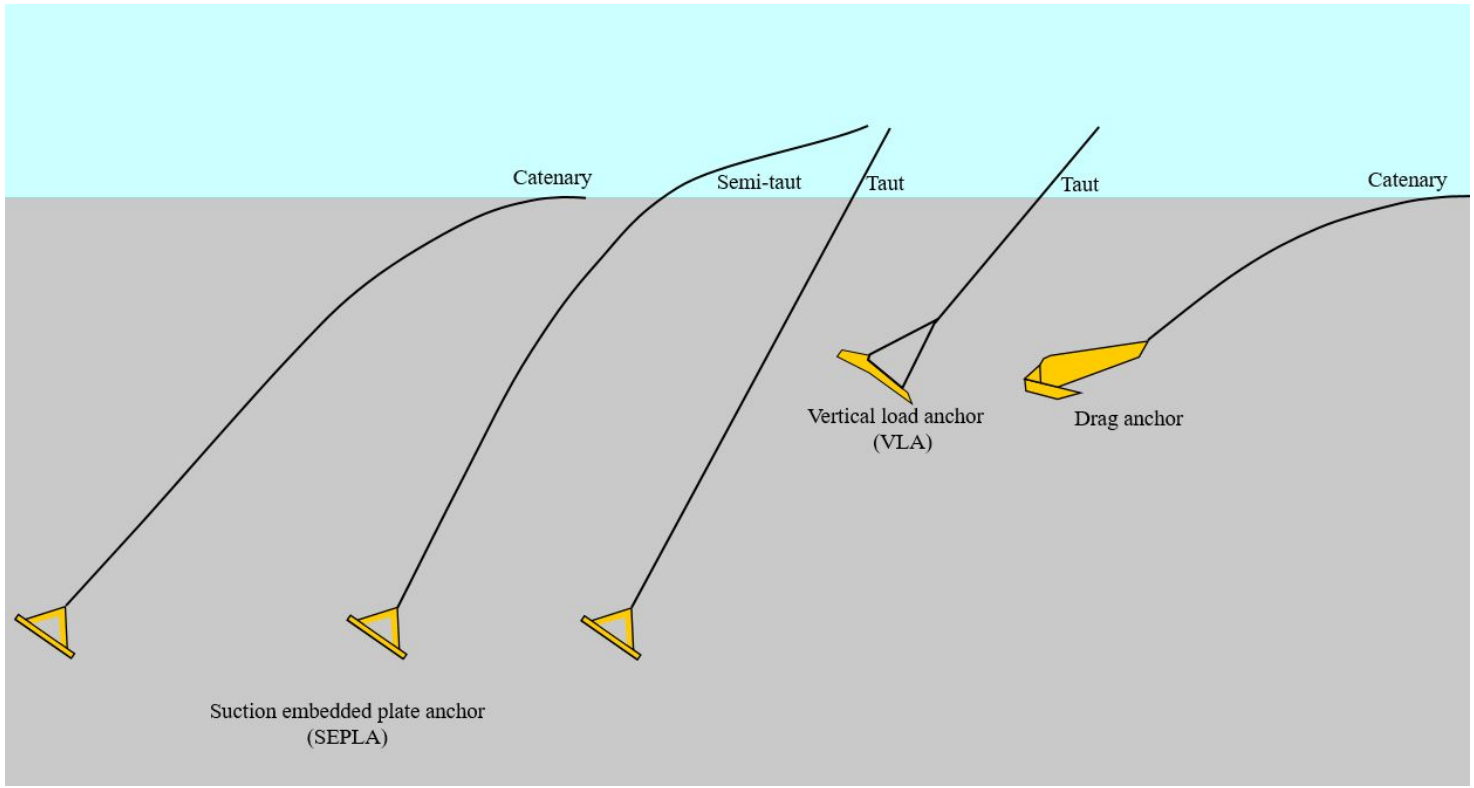


Figure 1 Offshore anchors and mooring systems

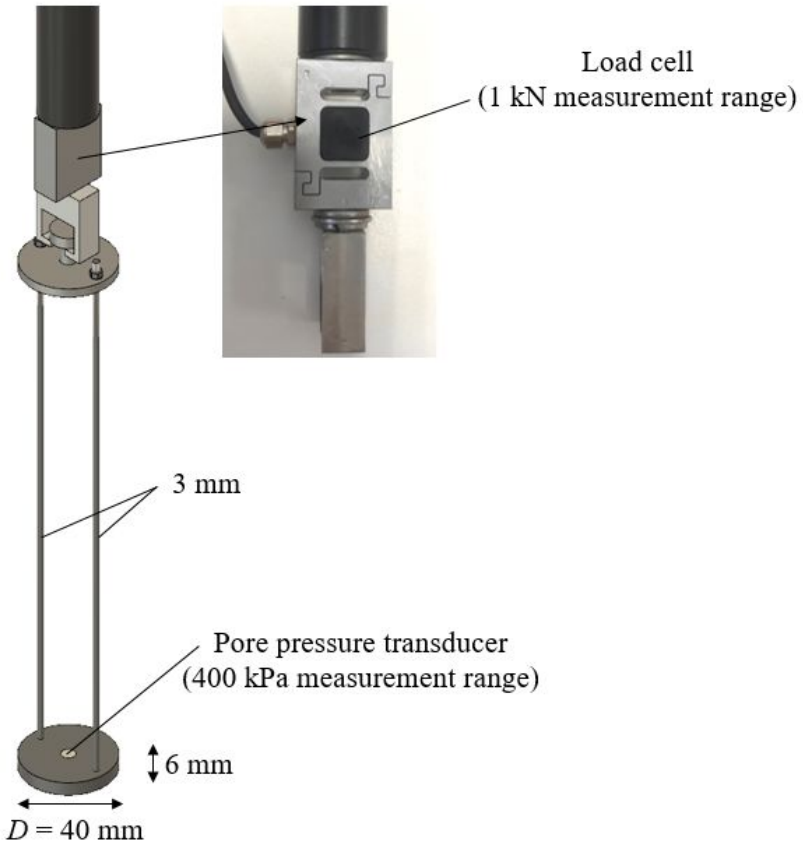


Figure 2 Model anchor and instrumentation

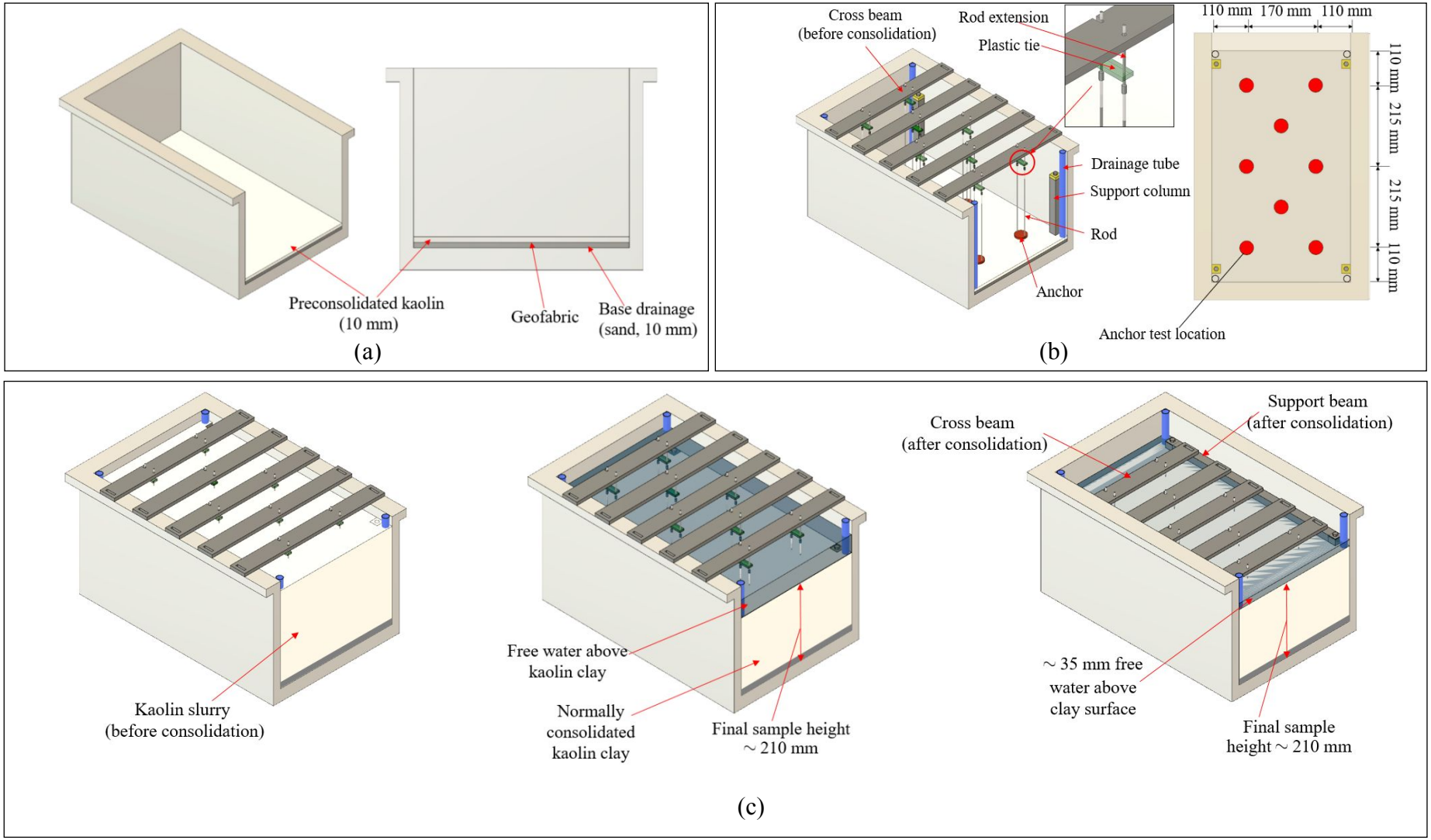


Figure 3 Sample preparation and anchor installation: (a) consolidation of lower clay layer; (b) anchor installation; (c) sample consolidation

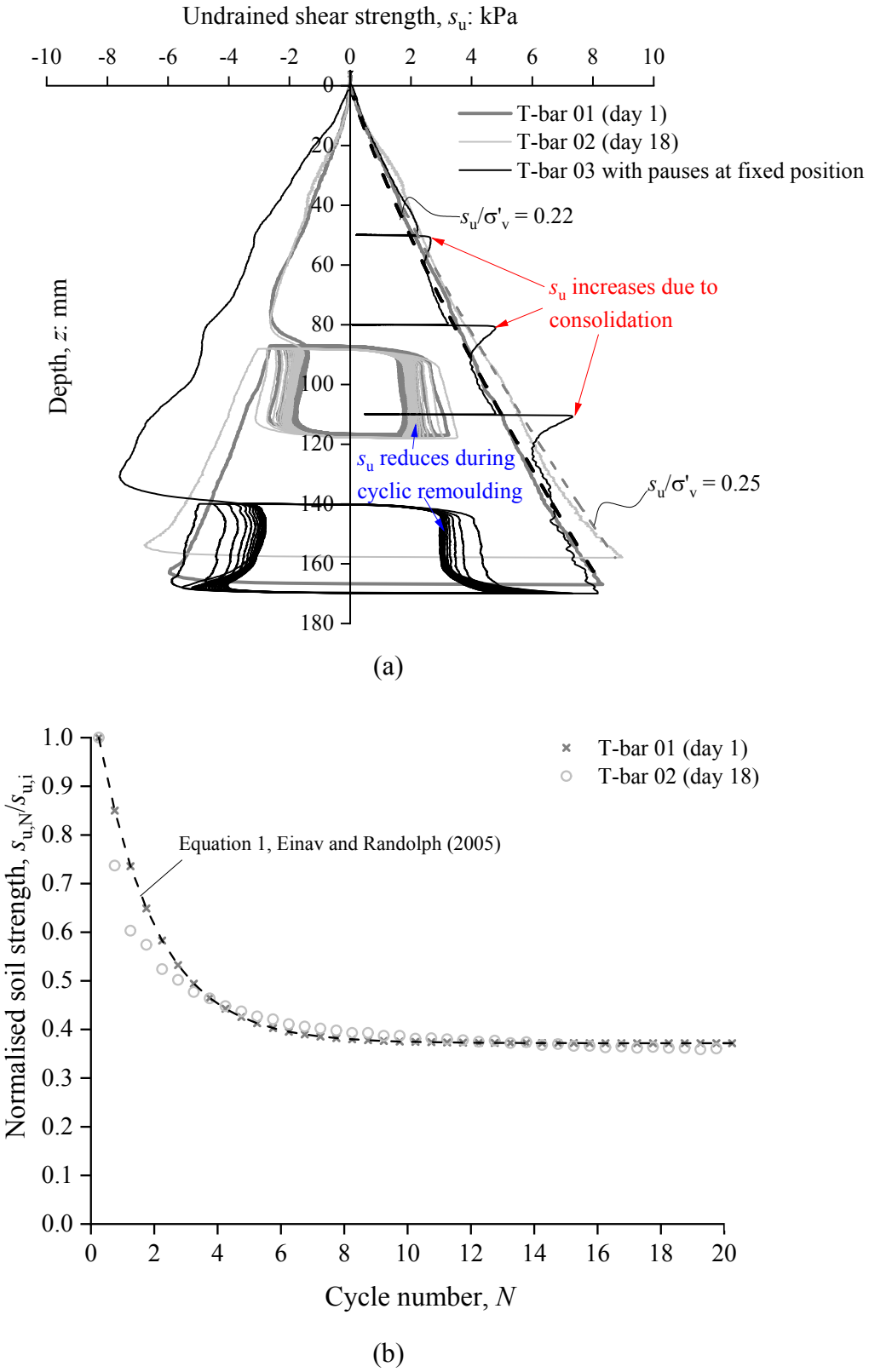


Figure 4 T-bar test data: (a) undrained shear strength profiles; (b) degradation in undrained shear strength during cyclic remoulding ($z$ = 105 mm)

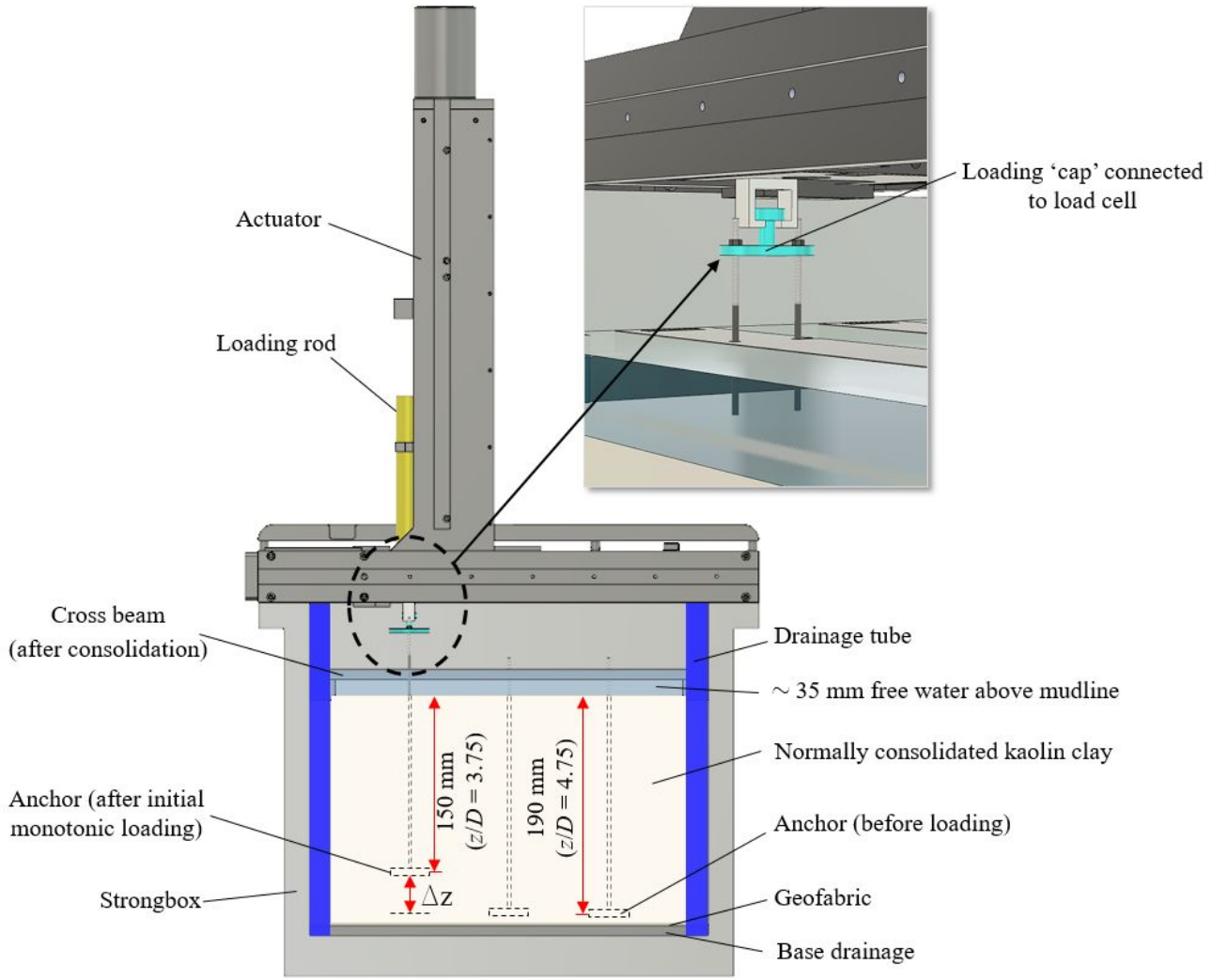


Figure 5 Experimental arrangement

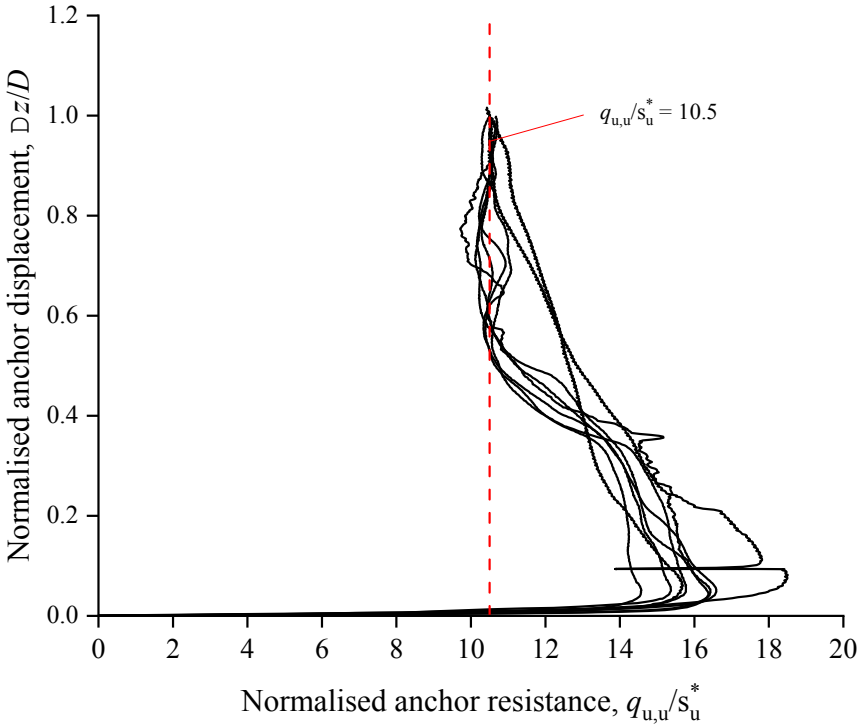


Figure 6 Anchor response during initial undrained monotonic loading

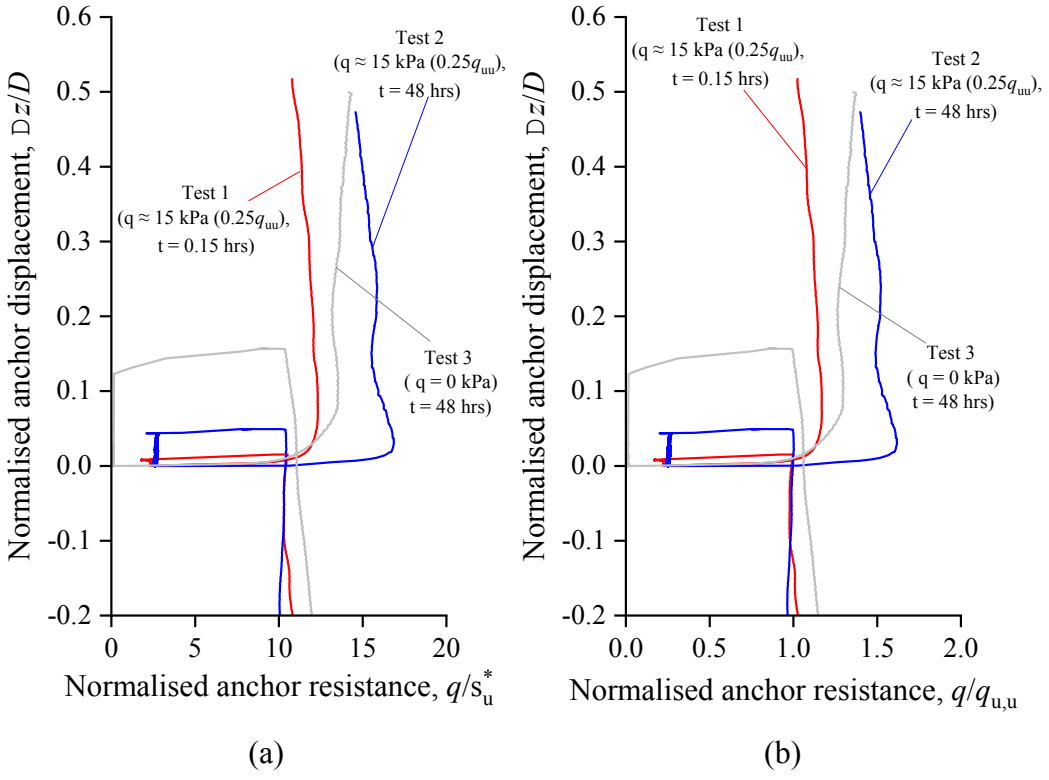


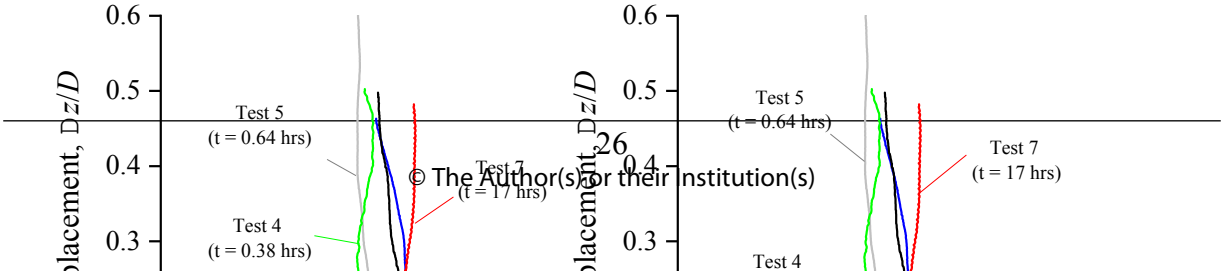

Figure 7 Anchor capacity increases after consolidation: (a) and (b) tests where the anchor resistance was fixed during consolidation; (c) and (d) tests where the anchor displacement was fixed during consolidation ((a) and (c) show anchor resistance normalised by undrained shear strength, whereas (b) and (d) show anchor resistance normalised by that at the end of the initial monotonic loading).

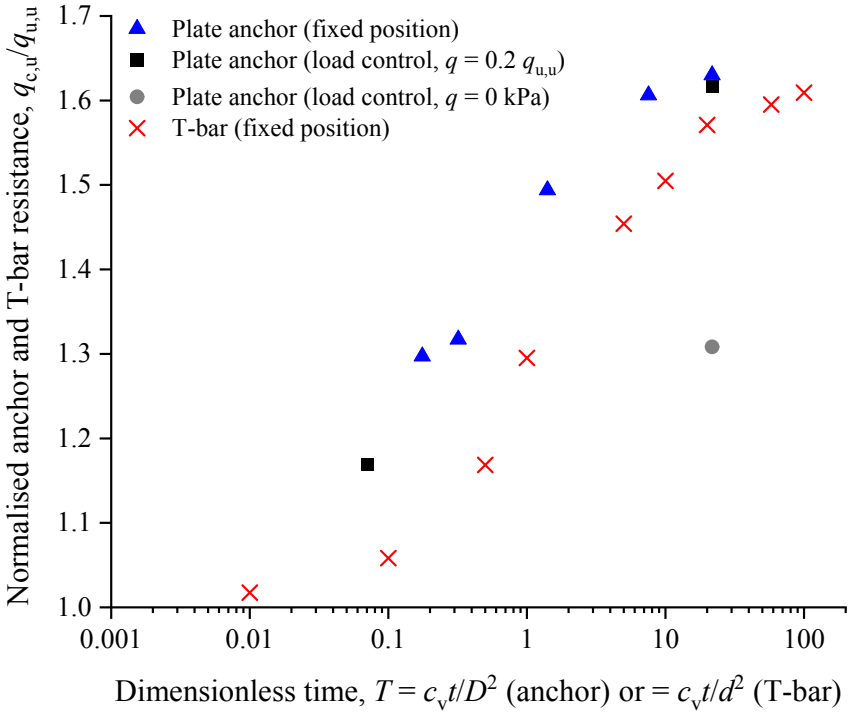


Figure 8 Changes in anchor capacity and soil strength after various consolidation periods

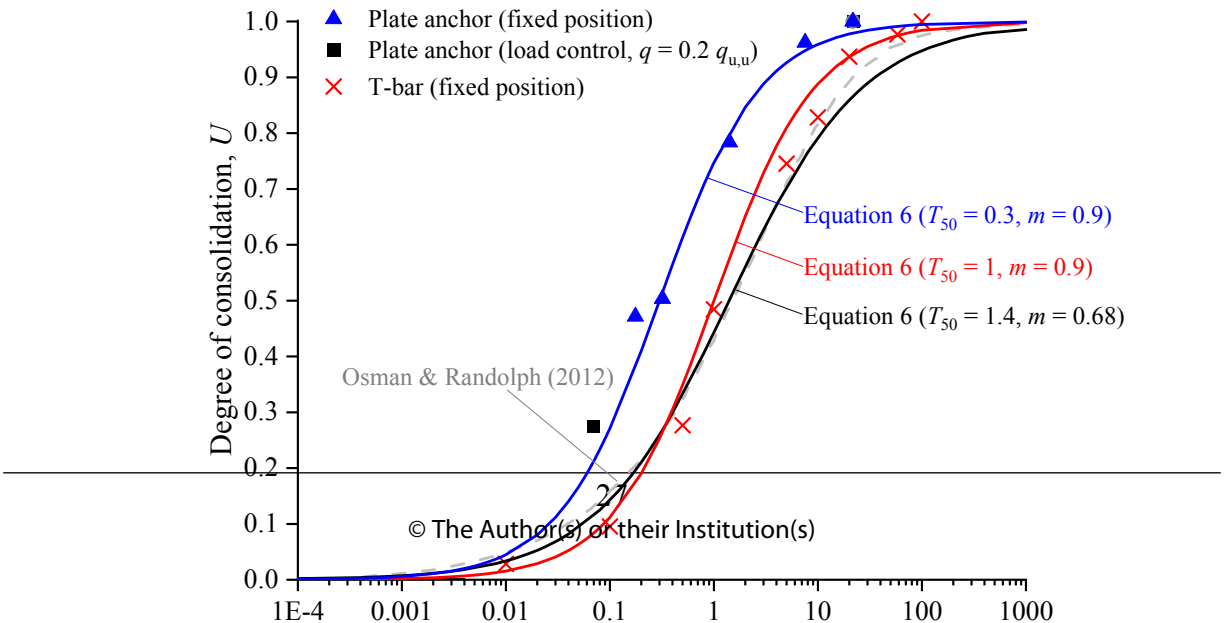

Figure 9 Degree of consolidation for anchor and T-bar tests

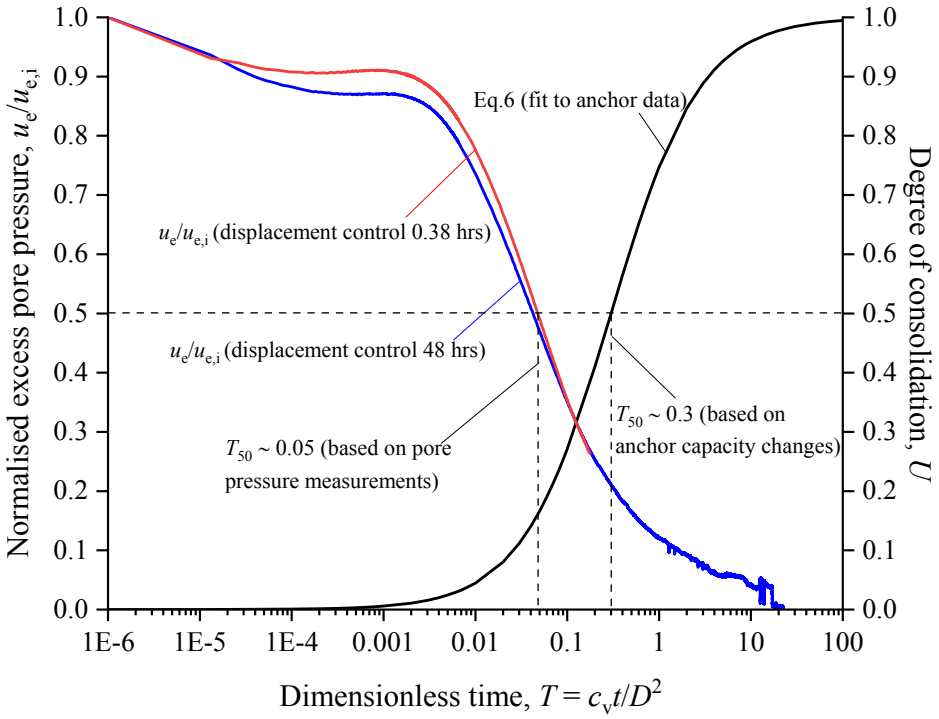


Figure 10 Consolidation progression as estimated from anchor capacity data and measured pore pressure response

Table 1 Geotechnical properties of Eckaolite kaolin clay

| Property | Value |
|---|---|
| Liquid limit, $w_{LL}$ (%) | 73.7 |
| Plastic limit, $w_{PL}$ (%) | 44.4 |
| Specific gravity, $G_s$ | 2.6 |
| Slope of normal consolidation line, λ | 0.435 |
| Slope of swelling line, κ | 0.044 |
| Coefficient of vertical consolidation, $c_v$ (m$^2$/year) [1] | 6.8 [2] |
| Effective unit weight, γ' (kN/m$^3$) [3] | 4.8 [2] |

[1] Assessed from one-dimensional consolidometer tests
[2] At the initial anchor depth, $\sigma'_v \approx 40$ kPa
[3] Assessed from moisture content determinations made on a sample core taken after the anchor tests.

Table 2 Test programme

| Test | Initial monotonic loading | | Consolidation stage | | | Post-consolidation monotonic loading | | Dimensionless anchor resistance | |
|---|---|---|---|---|---|---|---|---|---|
| | Displacement, $\Delta z$ (mm) | Penetration velocity, $v$ (mm/s) | Control | Consolidation duration, $t$ | Dimensionless time, $T = c_v t/D^2$ | Displacement, $\Delta z$ (mm) | Penetration velocity, $v$ (mm/s) | Initial, $q_{u,u}/s_u^*$ | After consolidation, $q_{c,u}/s_u^*$ |
| 1 | 40 | 0.75 | Fixed resistance, $q = 0.25q_{u,u}$ | 550 s | 0.07 | 20 | 0.75 | 10.54 | 12.33 |
| 2 | | | | 48 hrs | 21.71 | | | 10.42 | 16.84 |
| 3 | | | Fixed resistance, $q = 0$ kPa | 48 hrs | 21.71 | | | 10.44 | 13.57 |
| 4 | | | Fixed position | 1350 s | 0.176 | | | 10.50 | 13.62 |
| 5 | | | | 2300 s | 0.32 | | | 10.50 | 13.83 |
| 6 | | | | 3 hrs | 1.41 | | | 10.63 | 15.88 |
| 7 | | | | 17 hrs | 7.55 | | | 10.49 | 16.85 |
| 8 | | | | 48 hrs | 21.71 | | | 10.49 | 17.10 |